HHS Public Access

Author manuscript

Shock. Author manuscript; available in PMC 2017 January 01.

Published in final edited form as:

Shock. 2016 January ; 45(1): 88–97. doi:10.1097/SHK.0000000000000478.

AP39, a mitochondrially- targeted hydrogen sulfide donor, exerts protective effects in renal epithelial cells subjected to oxidative stress *in vitro* and in acute renal injury *in vivo*

Akbar Ahmad[1], **Gabor Olah**[1], **Bartosz Szczesny**[1,2], **Mark E. Wood**[3], **Matthew Whiteman**[4], and **Csaba Szabo**[1,2,*]

[1]Department of Anesthesiology, The University of Texas Medical Branch, Galveston, TX, USA [2]Shriners Hospital for Children, Galveston, TX, USA [3]Department of Biosciences, College of Life and Environmental Science, University of Exeter, England [4]University of Exeter Medical School, St. Luke's Campus, Exeter, England

Abstract

This study evaluated the effects of AP39 [(10-oxo-10-(4-(3-thioxo-3H-1,2-dithiol-5yl) phenoxy)decyl) triphenyl phosphonium bromide], a mitochondrially targeted donor of hydrogen sulfide (H_2S) in an *in vitro* model of hypoxia/oxidative stress injury in NRK-49F rat kidney epithelial cells (NRK cells) and in a rat model of renal ischemia-reperfusion injury. Renal oxidative stress was induced by the addition of glucose oxidase, which generates hydrogen peroxide in the culture medium at a constant rate. Glucose oxidase (GOx)-induced oxidative stress led to mitochondrial dysfunction, decreased intracellular ATP content, and, at higher concentrations, increased intracellular oxidant formation (estimated by the fluorescent probe 2, 7-dichlorofluorescein, DCF) and promoted necrosis (estimated by the measurement of lactate dehydrogenase release into the medium) of the NRK cells *in vitro*. Pretreatment with AP39 (30-300 nM) exerted a concentration-dependent protective effect against all of the above effects of GOx. Most of the effects of AP39 followed a bell-shaped concentration-response curve; at the highest concentration of GOx tested, AP39 was no longer able to afford cytoprotective effects. Rats subjected to renal ischemia/reperfusion responded with a marked increase (over 4-fold over sham control baseline) blood urea nitrogen and creatinine levels in blood, indicative of significant renal damage. This was associated with increased neutrophil infiltration into the kidneys (assessed by the myeloperoxidase assay in kidney homogenates), increased oxidative stress (assessed by the malondialdehyde assay in kidney homogenates) and an increase in plasma levels of IL-12. Pretreatment with AP39 (0.1, 0.2 and 0.3 mg/kg) provided a dose-dependent protection against these pathophysiological alterations; the most pronounced protective effect was observed at the 0.3 mg/kg dose of the H_2S donor; nevertheless AP39 failed to achieve a complete normalization of

*Corresponding author: szabocsaba@aol.com.

Competing interests: M.W., M.E.W. and the University of Exeter have intellectual property (patent filings) related to AP39 and its therapeutic uses. The other authors declare no conflicts of interest in relationship to this study.

Authors' contributions: Akbar Ahmad: conduction of experiments, analysis of data, preparation of manuscript; Gabor Olah: conduction of experiments, Bartosz Szczesny: conduction of experiments, Matthew Whiteman, Mark E. Wood: experimental design, preparation of manuscript; Csaba Szabo: experimental design, preparation of manuscript.

any of the injury markers measured. The partial protective effects of AP39 correlated with a partial improvement of kidney histological scores and reduced TUNEL staining (an indicator of DNA damage and apoptosis). In summary, the mitochondria-targeted H_2S donor AP39 exerted dose-dependent protective effects against renal epithelial cell injury *in vitro* and renal ischemia-reperfusion injury *in vivo*. We hypothesize that the beneficial actions of AP39 are related to the reduction of cellular oxidative stress, and subsequent attenuation of various positive feed-forward cycles of inflammatory and oxidative processes.

Keywords

oxidative stress; ischemia; renal injury; mitochondria; H_2S donor

Introduction

Renal ischemia followed by reperfusion (I/R), caused by circulatory shock of different etiologies, or by anesthesia, surgery, or transplantation, is a major cause of acute renal failure (ARF). The epithelial cells of the proximal tubule are particularly susceptible to I/R injury, leading to acute tubular necrosis, which plays a central part in the pathogenesis of ARF (1,2).

Over the last decade hydrogen sulfide (H_2S) emerged as an endogenously produced gaseous mediator, with anti-inflammatory and cytoprotective properties (3,4). Various H_2S donation strategies have been developed and tested *in vitro* and *in vivo* (5,6), including renal I/R injury. The goal of the current study was to evaluate the therapeutic effect of the mitochondrially targeted H_2S donor AP39 (7,8) in renal epithelial cells subjected to oxidative stress *in vitro* and in a rat model of renal ischemia *in vivo*. AP39 consists of a mitochondria-targeting motif, triphenyl phosphonium (TPP^+), coupled to a H_2S-donating moiety (dithiolethione) by an aliphatic linker. The purpose of the synthesis of this structure is to target H_2S delivery to the mitochondria, by exploiting the well-known property of TPP^+ to accumulate in mitochondria. The rationale of targeting the H_2S directly into the mitochondria follows recent observations that mitochondrial H_2S, at low concentrations exerts antioxidant, cytoprotective and stimulatory bioenergetic effects (5-9). We hypothesized that in renal oxidative injury, a process well known to be associated with mitochondrial dysfunction (10-12), a compound, which targets H_2S to mitochondria may exert therapeutic effects. The results of our current study show AP39 exerted significant and potent cytoprotective effects against hypoxia *in vitro* and against renal injury *in vivo*.

Materials & Methods

Materials

AP39 was synthesized in house as described (7). Other all chemicals were obtained from Sigma-Aldrich (St. Louis, MO, USA).

Cell culture

The NRK 49F cell line was purchased from the American Type Culture Collection (ATCC CRL#-1570), and cultured in Dulbecco's modified Eagle's medium (DMEM) containing glucose (1 g/l) and sodium pyruvate with 10% FBS, 4 mM L-glutamine adjusted to contain 1.5 g/l sodium bicarbonate, 100 IU/ml penicillin, 100 μg/ml streptomycin.

In vitro oxidative stress induced by glucose oxidase in the NRK cell model

NRK cells (20×10^3 cells per well) were seeded overnight onto 96-well tissue culture plates with cell culture medium and cultured at 37°C at 5% CO_2 atmosphere for 24 hours. After 24 hours, the cultured cells were washed with cell culture medium and pretreated with AP39 (30, 100 or 300 nM) followed by further incubation in the presence of cell culture medium for 30 minutes. To generate oxidative stress, we used glucose oxidase (GOx) (0.003, 0.03, 0.3 and 3 U/ml). In one set of studies we have used a short exposure (1 hour); in another set of studies we used 1h exposure with GOx, followed by a washout and a further incubation in the presence of tissue culture medium for 24 hours. At the end of the experiments, 3-(4,5-dimethylthiazol-2-yl)-2,5-diphenyltetrazolium bromide (MTT) viability assays, lactate dehydrogenase (LDH) cytotoxicity assay were performed. Cellular adenosine triphosphate (ATP) content and intracellular oxidant production was assessed as described below.

MTT assay

The MTT method was performed as described (8). Briefly, 3-(4,5-dimethyl-2-thiazolyl)-2,5-diphenyl-2H-tetrazolium bromide (MTT) was added to the cells at a final concentration of 0.5 mg/ml and cells were cultured at 37 °C for 1h. The cells were washed with PBS and the formazan dye was dissolved in DMSO. The amount of converted formazan dye was measured at 570 nm with a background measurement at 690 nm on a Powerwave reader (Biotek).

LDH assay

Measurement of lactate dehydrogenase (LDH) release into the medium (8) was used to assess the cytotoxicity of the H_2O_2 produced by GOx. Briefly, 30 μl of supernatant was saved before addition of MTT and mixed with 100 μl freshly prepared LDH assay reagent containing 85 mM lactic acid, 1 mM nicotinamide adenine dinucleotide (NAD^+), 0.27 mM N-methyl phenazonium methyl sulfate (PMS), 0.528 mM 2-(4-iodophenyl)-3-(4-nitrophenyl)-5-phenyl-2H-tetrazolium chloride (INT), and 200 mM Tris (pH 8.2). The changes in absorbance were read kinetically at 492 nm for 15min (kinetic LDH assay) on a monochromator-based reader (Powerwave HT, Biotek) at 37 °C. LDH activity values are shown as Vmax for kinetic assays in mOD/min.

Measurement of cellular ATP levels

Intracellular ATP concentration was determined by the commercially available CellTiter-Glo® Luminescent Cell Viability Assay (Promega, Madison, WI, USA) (13). Cells were lysed in 100 μL Cell Titer-Glo reagent according to the manufacturer's recommendations, and the luminescent signal was recorded for 1s on a high-sensitivity luminometer (Synergy 2; Biotek, Winooski, VT, USA). The assay is based on ATP requiring luciferin-oxyluciferin

conversion mediated by a thermostable luciferase that generates a stable “glow-type” luminescent signal.

2, 7-dichlorofluorescein (DCF) assay

Intracellular oxidant production was assessed using a commercially available Reactive Oxygen Species (ROS) Detection Reagent (Molecular Probes™, Invitrogen detection technologies, Eugene, OR, USA). At the end of the experiment, cells were then stained with 10 μM DCFH-DA for 30 minutes at 37°C and collected. After washing with phosphate-buffered saline (PBS), cells were resuspended in PBS followed by the determination of fluorescence intensity (λ excitation, 492-495 nm; λ emission, 517-527 nm) as described (14).

In vivo studies

All animal investigations confirm to the *Guide for the Care and Use of Laboratory Animals* published by the National Institutes of Health (NIH Publication No. 85-23, Revised 1985), and was approved by UTMB's local IACUC committee.

Male Sprague Dawley rats (12 weeks of age) were housed in a light-controlled room with a 12 hour light—dark cycle and were allowed ad libitum access to food and water. Rats were anesthetized with ketamine (100 mg/kg i.p.) & dexmedetomidine (0.15 mg/kg i.p.) and anesthesia was maintained by supplementary injections of one-third of the initial dose every 30 minutes.

Rats were randomly allocated into the following groups: (1) control + vehicle (n = 10); (2) I/R+vehicle (n =10); (3) I/R + AP39 (0.1 mg/kg, i.p.) 5 minutes before reperfusion (n = 10); (4) I/R+AP39 (0.2 mg/kg, i.p.) 5 minutes before reperfusion (n = 12) and (5) I/R+AP39 (0.3mg/kg, i.p.) 5 minutes before reperfusion. The volume of saline (V) administered to the control animals was equal to the volume of AP39 administered.

The animals were anesthetized as detailed above. After performing a midline laparotomy, animals were subjected to bilateral renal ischemia for 30 minutes, during which the renal arteries and veins were occluded using microaneurysm clamps. The time of ischemia was set in order to maximize the reproducibility of the renal functional impairment while minimizing mortality. Treatment groups received vehicle or AP39 (0.1, 0.2 or 0.3 mg/kg) 5 minutes before onset of reperfusion. After the renal clamps was removed, the kidneys were observed for a further 5 minutes to ensure reflow, after which 500 μl of saline at 37°C was injected into the abdomen, and the incision was sutured. At 6 hours after reperfusion, animals were euthanized under deep anesthesia by using isoflurane (5% inhalation) and death was confirmed by opening of chest. Blood and kidneys were collected for evaluation (15). Control animals underwent identical surgical procedures but without bilateral renal pedicle clamping and were subjected to all procedures used in the other three groups.

Measurement of plasma BUN and creatinine levels

At the end of the reperfusion period, rats were sacrificed, and blood samples (1 ml) were collected via cardiac puncture. The blood samples (100 microliter) were analyzed by a

Vetscan analyzer for biochemical parameters (BUN & creatinine) within 1 hour of collection as described (16).

Determination of tissue lipid peroxidation using the malondialdehyde assay

Tissue malondialdehyde (MDA) levels, an index of cellular injury/oxidative stress (17), were detected in kidney samples using a fluorimetric MDA-specific lipid peroxidation assay kit (Enzo Life Sciences, Farmingdale, NY, USA) according to the manufacturer's instructions. The assay is based on the BML-AK171 method in which two molecules of the chromogenic reagent N-methyl-2-phenylindole (NMPI) react with one molecule of MDA at 45°C to yield a stable carbocyanine dye with a maximum absorption at 586 nm.

Determination of tissue neutrophil infiltration using the myeloperoxidase activity assay

Myeloperoxidase activity was measured in kidney samples using a commercially available myeloperoxidase (MPO) fluorimetric detection kit (Enzo Life Sciences) (17). The assay utilizes a non-fluorescent detection reagent, which is oxidized in the presence of H_2O_2 and MPO to produce its fluorescent analog. The fluorescence was measured at excitation wavelength of 530 nm and emission wavelength of 590 nm.

Measurement of plasma cytokine levels

Blood from all groups was collected in K_2EDTA blood collection tubes and centrifuged at 4°C for 15 minutes at 2,000 × g within 30 minutes of collection. Plasma was isolated, aliquoted and stored at −80 °C until use. The EMD Millipore's MILLIPLEX™ MAP Mouse cytokine Magnetic Bead Panel 1 kit was used for the quantification of TNF-α, IFN-γ, GM-CSF, IL-1α, IL-1β, IL-2, IL-4, IL-6, IL-10 and IL-12 (Merck Millipore, Darmstadt, Germany) (16). Data analysis was performed using the Luminex xPONENT™ acquisition software (Thermo Fisher Scientific, Waltham, MA, USA).

Histological studies and TUNEL assay

Kidney biopsies were taken at 6 hours after reperfusion. The biopsies were fixed for 1 week in buffered formaldehyde solution (10% in PBS) at room temperature, dehydrated by graded ethanol and embedded in Paraplast (Sherwood Medical, Mahwah, NJ, USA). Tissue sections (thickness: 7 μm) were deparaffinized with xylene stained with hematoxylin/eosin and studied using light microscopy. Histological studies were performed in a blinded fashion. In the *in vivo* model, a TUNEL assay was performed by an evaluator who was blinded to the treatment animals had received. The TUNEL assay was conducted using a TUNEL detection kit (ApopTag Peroxidase *In Situ* Apoptosis Detection Kit) according to the manufacturer's instruction (EMD Millipore, CA, USA).

Statistical analysis

All values described in the text and figures are expressed as means ± SEM for *n* observations. Student's t-test, one-way and two-way ANOVA with Tukey's post hoc test were used to detect differences between groups; Prism version 5 for Windows (GraphPad Software). $p<0.05$, $p<0.01$ were considered statistically significant.

Results

Effect of AP39 on the MTT converting ability of NRK cells exposed to oxidative stress by GOx

Exposure of the cells to glucose oxidase (0.003, 0.03, 0.3 or 3 U/ml) for 1 hour (Figure 1A) or, in another set of studies, incubation with glucose oxidase for 1 hour, followed by a washout, and followed by a further 24h incubation period (Figure 1B), resulted in a concentration-dependent decrease in cellular viability, evidenced by suppressed MTT conversion (Figures 1A & B). When lower concentrations of GOx (0.003 U/ml or (0.03 U/ml) were used, pretreatment with the lowest concentration of AP39 (30 nM) enhanced the cellular viability of the NRK cells; the decrease in MTT conversion in GOx treated cells was attenuated by AP39, while elevation of the AP39 concentration to 100 or 300 nM no longer exerted protective effects against the GOx induced decreases in MTT conversion, suggestive of a bell-shaped concentration-response curve. When a higher concentration of GOx was used (0.3 U/ml), 30 nM AP39 failed to protect, while the ‘peak’ of the bell-shaped concentration-response curve was found at the concentration of 100 nM AP39 (Figures 1A & B). Moreover, AP39-mediated protection was only observed at intermediate concentrations of GOx; the protective effects were no longer observed against the decrease in MTT conversion elicited by the highest concentrations (3 U/ml) of GOx used.

Effect of AP39 on LDH release of NRK cells exposed to oxidative stress by GOx

The effect of AP39 was also tested on the breakdown of the integrity of the plasma membrane, as measured by LDH release into the extracellular medium, both in the short-term exposure to GOx (Figure 2A) as well as in the experiment where GOx exposure was followed by a washout and a 24h further incubation (Figure 2B). AP39 (30, 100 or 300 nM) reduced the release of LDH at all concentrations of GOx. When higher concentration of GOx was used (0.3 U/ml), 30 nM AP39 failed to protect, while the ‘peak’ of the bell-shaped concentration-response curve was found at the concentration of 100 nM AP39 (Figure 2B). The protective effects were less pronounced with the highest concentration (300 nM) of AP39, than with the lower concentrations, consistent with a bell-shaped concentration-response curve. Interestingly, although AP39 failed to protect against the suppression of MTT conversion at the highest flux of reactive oxygen species elicited in our study (by the highest concentration of GOx used), the results showed that AP39 (most pronouncedly at 30 and 100 nM; less pronouncedly at 300 nM) afforded partial protection against the GOx-induced LDH release under the same experimental conditions (Figures 2A & B).

Effect of AP39 on the ATP content of NRK cells exposed to oxidative stress by GOx

ATP levels in NRK cells exposed to GOx in the presence and absence of AP39 (30-300 nM) were also determined (Figures 3A & B). AP39 inhibited GOx-induced depletion of ATP. However, the protective effects of AP39 on ATP levels were not apparent at the highest concentration of GOx employed (3 U/ml).

Effect of AP39 on the intracellular oxidant production in NRK cells exposed to GOx

At the two highest concentrations tested, GOx produced a marked increase in DCF fluorescence, both in the acute exposure (Figure 4A) and in the GOx exposure/washout/24h incubation experiments (Figure 4B). Because in the latter conditions GOx was no longer in the medium, DCF fluorescence indicates a secondary, endogenous oxidant production (which was triggered by the initial oxidant exposure generated by GOx). AP39 (30, 100 and 300 nM) reduced GOx-induced intracellular oxidant production however the 'bell-shaped' response observed in other assays (e.g. ATP, LDH, MTT) was not observed.

Effect of AP39 on tissue injury in a renal ischemia-reperfusion (I/R) model in rats

Renal ischemia (30 minutes), followed by reperfusion (6 hours) significantly impaired glomerular function, as evidenced by markedly increased (over 4-fold over sham control baseline) blood urea nitrogen (Figure 5A) and creatinine levels (Figure 5B). Renal I/R damage was dose-dependently reduced by AP39; the most pronounced (nevertheless, only partial) protection was noted at the 0.3 mg/kg dose of the H_2S donor.

Effect of AP39 on renal MPO and MDA levels in a renal ischemia-reperfusion model in rats

MDA, an index of oxidative stress, was significantly increased in the renal ischemia/reperfusion group, compared to the sham control group; and these increases were partially attenuated by pretreatment of the rats with AP39 in dose-dependent manner (Figure 6A). Similarly, AP39 attenuated renal MPO levels, an index of neutrophil infiltration (Figure 6B).

Effect of AP39 on plasma cytokine levels in a renal ischemia-reperfusion model in rats

Plasma levels of TNF-α, IFN-γ, GM-CSF, IL-1α IL-1β, IL-2, IL-4, IL-6 and IL-10 were unaffected by ischemia-reperfusion, as measured at the end of the experiments (6 hours after reperfusion); respective sham-control and post-ischemia-reperfusion values amounted to 24.2±0.5 and 26.2±2.1 for TNF-α 46.3±0.3 and 45.1±0.4 for IFN-γ, 13.2±0.9 and 14.1±0.5 for GM-CSF, 20.1±1.0 and 20.0±1.7 for IL-1α 37.1±1.2 and 35.4±1.7 for IL-1β, 54.8±2.3 and 55.1±3.2 for IL-2, 13.1±0.3 and 13.1±0.6 for IL-4, 20.4±0.9 and 19.9±1.3 for IL-6 and 20.1±1.1 and 19.3±0.8 for IL-10 (all values in pg/ml; n=10). IL-12 were significantly increased in the renal ischemia-reperfusion, group compared to the control group (Figure 7). This increase was dose-dependently attenuated by AP39 (Figure 7); most pronouncedly at the 0.3 mg/kg dose of the H_2S donor.

Effect of AP39 on histopathology and apoptosis of the renal tissue in a renal ischemia-reperfusion model in rats

Hematoxylin and eosin–stained sections are from the outer medulla (representative images of at least three experiments), are shown in Figure 8A. Neutrophil accumulation within the interstitium of the kidney was induced by ischemia-reperfusion; this effect was attenuated in AP39 (0.3 mg/kg) treated rats. AP39-treated rats subjected to renal I/R, nevertheless, remained to show a significant degree of injury (evidenced by a loss of glomerular integrity and swollen epithelium), although to a lesser degree than the degree of injury seen in the I/R group that did not receive AP39. In the renal ischemia and reperfusion group TUNEL positive cells were also observed in the kidney tissue within 6h and the number of TUNEL

positive cells was significantly reduced by treatment of the animals with AP39 (0.3 mg/kg) (Figure 8B).

Discussion

Inhibition of cytochrome C oxidase (mitochondrial Complex IV) is the longest known mitochondrial effect of H_2S (18). This effect has been proposed to underlie most of the toxic effects of high-dose H_2S exposure, and it is the prominent mechanism of toxicity in the toxicological literature. However, Bouillaud et al. have shown that H_2S, at lower concentrations, acts as an electron donor to the mitochondria, and serves as an inorganic substrate for mitochondrial electron transport (19,20); the phenomenon also exists when H_2S is produced by endogenous (intramitochondrial) enzymatic sources (21). These effects are intriguing since mitochondria endogenously produce H_2S under physiological conditions or from CSE (after its mitochondrial translocation) in cells exposed to hypoxia (22) or from CBS (for instance in colon cancer cells and ovarian cancer cells) (23). Additional mitochondrial stimulatory/protective effects of H_2S include the stimulation of mitochondrial electron transport via inhibition of mitochondrial phosphodiesterase 2A, followed by elevation of intramitochondrial cAMP levels (24) and the activation of mitochondrial Complex V (ATP synthase) via sulfhydration (25). In addition to these specific reactions, H_2S has also been demonstrated to form an overall antioxidative protective environment within the mitochondrion, which reduces mitochondrial oxidant production, maintains mitochondrial integrity and protects the mitochondria against various forms of oxidative stress (26,27).

Considering to the above listed beneficial mitochondrial properties of H_2S, the idea of pharmacological mitochondrial targeting of H_2S has emerged in recent years (7,8,28,29). The mitochondrially targeted donor AP39 (7) has been shown to increase H_2S levels within the mitochondrial compartment of endothelial cells (8); has been shown to exert bell-shaped effects on mitochondrial electron transport (stimulation at low concentration, followed by inhibition at higher concentrations); has been shown to exert protective effects in endothelial cells against oxidative stress, including maintenance of mitochondrial function, protection of mitochondrial DNA integrity and inhibition of mitochondrial protein oxidation (8). Moreover, AP39 has been shown to exert hemodynamic effects (e.g. reduction in blood pressure) *in vivo* (28) (consistently with the hemodynamic effects of authentic H_2S) and has shown potent neuroprotective effects in mice after cardiac arrest / CPR at doses 3 orders of magnitude lower than authentic, and non-mitochondrial, H_2S (29). Our current finding that AP39 protected kidney epithelial cells against oxidative stress *in vitro* and protected the kidney against ischemia-reperfusion injury adds to the above list of conditions where H_2S and, in particular, H_2S delivered to mitochondria using a TPP^+-based approach exerts beneficial effects. Importantly, the dose of the AP39 in the above studies is substantially lower than the dose of the ‘traditional’ non-targeted H_2S donors (e.g. NaHS) previously shown to exert protective effects.

In the *in vitro* experiments utilizing NRK kidney epithelial cells, four different, but related parameters (MTT conversion, LDH release, ATP content and cellular ROS generation) were measured, in an acute setting (one hour of glucose oxidase exposure) and in an acute

exposure/washout/24 hours follow-up setting which may be considered, in some respects, an *in vitro* model of ischemia/reperfusion. The protective effect of AP39 was most apparent at 30 and 100 nM, which is the same concentration range used by us previously and found to protect vascular endothelial cells from oxidative damage, and which was the basis for selecting the concentrations to be used for the experimental design of the current study (8). According to simplified models of oxidative cell injury, all of the four parameters represent "injury markers" (MTT indicates mitochondrial function, LDH indicates the breakdown of cell membrane permeability and cell necrosis, ATP levels are decreased when mitochondrial function of the cell is impaired, and intracellular oxidants are generated by dysfunctional mitochondria, as well as various other sources in a stressed/dying cell). There were some findings that support the above outlined simplistic model, and there were some significant differences in the pattern of these alterations, and the ability of AP39 to protect against them, that would argue for a more complex model. For example, the decreases in cell viability (e.g. measured using the MTT assay) (Figure 1) are already apparent at GOx concentrations that were not yet able to induce LDH release (an indicator of the breakdown of the cell membrane's integrity) (Figure 2), nor intracellular oxidant production (Figure 4), nor a significant decrease in cellular ATP content (Figure 3). This finding also indicates that intracellular oxidants, secondary to the initial 1 hour of GOx exposure may not be the primary cause of cell death in this model.

Overall, the results presented in Figures 1-4 are consistent with the suggestion that the effects of AP39 (similar to the effects of authentic H_2S in a variety of models) follow a bell-shaped concentration-response curve; AP39 concentrations of 30 nM and 100 nM exerted most of the protective effects, and 300 nM being less effective. In some experimental conditions and for some read-out parameters - e.g. the MTT conversion data shown in Figure 1A, when cells were challenged with 0.003 U/ml glucose oxidase - 30 nM AP39 exerted the most protective effects, and increasing its concentration was no longer effective. In other experimental conditions (e.g. - the MTT conversion data shown Figures 1A &B, when cells were challenged with 0.3 U/ml, a substantially higher flux of ROS), 30 nM AP39 was not (yet) effective; the protection afforded by AP39 peaked at 100 nM, and, once again, further increasing its concentration to 300 nM was no longer protective. These findings suggest that the effective concentration of AP39, while, under our experimental conditions, always tends to be in the low-to-mid nM range. However, the actual 'peak' of the bell-shaped curve is a function of the oxidant flux that the cells are exposed to. In fact, in some of the experimental conditions, inclusion of AP39 concentration(s) lower than 30 nM would have been useful to find the lower threshold of the protective effect. Nevertheless, taken the totality of the data presented in the current study, as well as the results of a previous study conducted in endothelial cells exposed to oxidative stress (8) are consistent with the conclusion that AP39 exerts cytoprotective effects at low-to-mid nanomolar concentrations and exhibits a bell-shaped concentration-response curve.

Interestingly, the marked decrease in MTT conversion at 3 U/ml GOx (the highest concentration of GOx used in the current study) and the marked decrease in cellular ATP content in the same conditions, would suggest that this high degree of oxidative stress generated under such conditions is too overwhelming and no longer influenced by a H_2S

donor. However, interestingly, even at the 3 U/ml GOx concentration, AP39 (most pronouncedly at 100 and 300 nM) continued to provide a partial protection against the LDH release. This finding although unexpected, indicates that the different viability read-outs (e.g. decreases in MTT being indicators of the ROS-mediated suppression of mitochondrial respiration and increases in LDH being indicators of the breakdown of cell membrane potential and the start of leaking of the intracellular content to the extracellular space) have a different sensitivity threshold and different responsiveness to H_2S. We speculate that some amount of H_2S, produced by the AP39, may reach extramitochondrial (i.e. cytoplasmatic or cell membrane) targets; this is especially likely at the high fluxes of GOx, because at these experimental conditions the high ROS flux is likely to dissipate the mitochondrial membrane potential (which is the driving force for the accumulation of the TPP-targeting groups of AP39 in the mitochondria in the first place). Under such conditions, it is conceivable (although remains to be explored) that the H_2S that is generated by AP39 affects secondary (non-mitochondrial targets), which could have contributed to the protection of cell membrane integrity. These possibilities and mechanisms remain to be explored in further studies.

In the *in vivo* studies, AP39 produced a dose-dependent protective effect against all parameters of renal ischemia-reperfusion injury tested (plasma markers of renal dysfunction, renal oxidative stress, renal infiltration of mononuclear cells, as well as plasma levels of IL-12). These protective effects of AP39 may be related to cytoprotection of the kidney against oxidative stress - a hallmark and significant causative factor in renal ischemia-reperfusion injury (1,2); in fact, the protective effect of AP39 against epithelial oxidative injury (present study) and endothelial injury (7,8) supports this notion. The exact mechanism by which IL-12 levels are reduced by AP39 are not yet clear, but it is possible that AP39 interferes with positive feedback cycles of ischemia/reperfusion injury, oxidant production, and pro-inflammatory signaling. The pathogenetic role of IL-12 in renal ischemia-reperfusion injury has been studied in several prior experiments. For example, IL-12 has been proposed to enhance and upregulate other pro-inflammatory mediators, which, in turn, would be expected to exacerbate renal dysfunction (30); in fact, there is evidence for a Th1/Th2 switched immune response in the pathogenesis of renal ischemia-reperfusion injury (30). In addition, neutralization of IL-12 has been shown to exert limited protective effects in a renal ischemia-reperfusion model (31,32). Thus, it is likely that IL-12 is an effector, rather than merely a general marker of renal ischemia-reperfusion injury. It remains to be directly tested to what extent the *in vivo* protection by AP39 in I/R involves modulation of IL-12 production, and whether AP39 modulates of Th1/Th2 responses in I/R and in other pathophysiological conditions.

The current study, coupled with prior studies showing that exogenous or endogenous H_2S can protect kidney epithelial cells *in vitro* and kidney from various forms of ischemic and toxic insults *in vivo* (33-35) supports the view that H_2S donation is a potential therapeutic approach to preserve renal function.

Acknowledgments

This work was supported by the National Institutes of Health (R01GM107846) to C.S.

References

1. Paller MS. The cell biology of reperfusion injury in the kidney. J Invest Med. 1994; 42:632–639.
2. Kribben A, Edelstein CL, Schrier RW. Pathophysiology of acute renal failure. J Nephrol. 1999; 12:s142–s151. [PubMed: 10688414]
3. Szabo C. Hydrogen sulphide and its therapeutic potential. Nat Rev Drug Discov. 2007; 6:917–935. [PubMed: 17948022]
4. Wallace JL, Wang R. Hydrogen sulfide-based therapeutics: exploiting a unique but ubiquitous gasotransmitter. Nat Rev Drug Discov. 2015; 14:329–345. [PubMed: 25849904]
5. Szabo C. Medicinal chemistry and therapeutic applications of the gasotransmitters nitric oxide, carbon monoxide and hydrogen sulfide. Burger's Medicinal Chemistry. 2010; 5:265–367.
6. Martelli A, Testai L, Breschi MC, Blandizzi C, Virdis A, Taddei S, Calderone V. Hydrogen sulphide: novel opportunity for drug discovery. Med Res Rev. 2012; 32:1093–1130. [PubMed: 23059761]
7. Trionnaire SL, Perry A, Szczesny B, Szabo C, Winyard PG, Whatmore JL, Wood ME, Whiteman M. The synthesis and functional evaluation of a mitochondria-targeted hydrogen sulfide donor, (10-oxo-10-(4-(3-thioxo-3H-1,2-dithiol-5-yl)nphenoxy) decyl)triphenylphosphonium bromide (AP39). Med Chem Commun. 2014; 5:728–736.
8. Szczesny B, Módis K, Yanagi K, Coletta C, Le Trionnaire S, Perry A, Wood ME, Whiteman M, Szabo C. AP39, a novel mitochondria-targeted hydrogen sulfide donor, stimulates cellular bioenergetics, exerts cytoprotective effects and protects against the loss of mitochondrial DNA integrity in oxidatively stressed endothelial cells in vitro. Nitric Oxide. 2014; 41:120–130. [PubMed: 24755204]
9. Szabo C, Ransy C, Módis K, Andriamihaja M, Murghes B, Coletta C, Olah G, Yanagi K, Bouillaud F. Regulation of mitochondrial bioenergetic function by hydrogen sulfide. Part I Biochemical and physiological mechanisms. Br J Pharmacol. 2014; 171:2099–2122. [PubMed: 23991830]
10. Versteilen AM, Di Maggio F, Leemreis JR, Groeneveld AB, Musters RJ, Sipkema P. Molecular mechanisms of acute renal failure following ischemia/reperfusion. Int J Artif Organs. 2004; 27:1019–1029. [PubMed: 15645611]
11. Tirapelli LF, Bagnato VS, Tirapelli DP, Kurachi C, Barione DF, Tucci S Jr, Suaid HJ, Cologna AJ, Martins AC. Renal ischemia in rats: mitochondria function and laser autofluorescence. Transplant Proc. 2008; 40:1679–1684. [PubMed: 18589172]
12. Hall AM, Rhodes GJ, Sandoval RM, Corridon PR, Molitoris BA. In vivo multiphoton imaging of mitochondrial structure and function during acute kidney injury. Kidney Int. 2013; 83:72–83. [PubMed: 22992467]
13. Szoleczky P, Módis K, Nagy N, Dóri Tóth Z, DeWitt D, Szabó C, Gero D. Identification of agents that reduce renal hypoxia-reoxygenation injury using cell-based screening: purine nucleosides are alternative energy sources in LLC-PK1 cells during hypoxia. Arch Biochem Biophys. 2012; 517:53–70. [PubMed: 22100704]
14. Brunyanszki A, Olah G, Coletta C, Szczesny B, Szabo C. Regulation of mitochondrial poly(ADP-Ribose) polymerase activation by the β-adrenoceptor/cAMP/protein kinase A axis during oxidative stress. Mol Pharmacol. 2014; 86:450–462. [PubMed: 25069723]
15. Di Paola R, Genovese T, Impellizzeri D, Ahmad A, Cuzzocrea S, Esposito E. The renal injury and inflammation caused by ischemia-reperfusion are reduced by genetic inhibition of TNF-αR1: a comparison with infliximab treatment. Eur J Pharmacol. 2013; 700:134–146. [PubMed: 23291313]
16. Coletta C, Módis H, Oláh G, Brunyánszki A, Herzig DS, Sherwood ER, Ungvári Z, Szabo C. Endothelial dysfunction is a potential contributor to multiple organ failure and mortality in aged mice subjected to septic shock: preclinical studies in a murine model of cecal ligation and puncture. Crit Care. 2014; 18:511. [PubMed: 25223540]
17. Soriano FG, Lorigados CB, Pacher P, Szabó C. Effects of a potent peroxynitrite decomposition catalyst in murine models of endotoxemia and sepsis. Shock. 2011; 35:560–566. [PubMed: 21263378]
18. Nicholls P, Marshall DC, Cooper CE, Wilson MT. Sulfide inhibition of and metabolism by cytochrome c oxidase. Biochem Soc Trans. 2013; 41:1312–1316. [PubMed: 24059525]

19. Goubern M, Andriamihaja M, Nübel T, Blachier F, Bouillaud F. Sulfide, the first inorganic substrate for human cells. FASEB J. 2007; 21:1699–1706. [PubMed: 17314140]
20. Abou-Hamdan A, Guedouari-Bounihi H, Lenoir V, Andriamihaja M, Blachier F, Bouillaud F. Oxidation of H_2S in mammalian cells and mitochondria. Methods Enzymol. 2015; 554:201–228. [PubMed: 25725524]
21. Módis K, Coletta C, Erdélyi K, Papapetropoulos A, Szabo C. Intramitochondrial hydrogen sulfide production by 3-mercaptopyruvate sulfurtransferase maintains mitochondrial electron flow and supports cellular bioenergetics. FASEB J. 2013; 27:601–611. [PubMed: 23104984]
22. Fu M, Zhang W, Wu L, Yang G, Li H, Wang R. Hydrogen sulfide (H_2S) metabolism in mitochondria and its regulatory role in energy production. Proc Natl Acad Sci USA. 2012; 109:2943–2948. [PubMed: 22323590]
23. Szabo C, Coletta C, Chao C, Módis K, Szczesny B, Papapetropoulos A, Hellmich MR. Tumor-derived hydrogen sulfide, produced by cystathionine-β-synthase, stimulates bioenergetics, cell proliferation, and angiogenesis in colon cancer. Proc Natl Acad Sci USA. 2013; 110:12474–12479. [PubMed: 23836652]
24. Módis K, Panopoulos P, Coletta C, Papapetropoulos A, Szabo C. Hydrogen sulfide-mediated stimulation of mitochondrial electron transport involves inhibition of the mitochondrial phosphodiesterase 2A, elevation of cAMP and activation of protein kinase A. Biochem Pharmacol. 2013; 86:1311–1319. [PubMed: 24012591]
25. Módis K, Altaany Z, Untereiner A, Yang G, Wu L, Wang R, Szabo C. Hydrogen sulfide-induced S-sulfhydration of ATP synthase stimulates mitochondrial bioenergetics. Nitric Oxide. 2015; 47:S53–S54.
26. Suzuki K, Olah G, Modis K, Coletta C, Kulp G, Gerö D, Szoleczky P, Chang T, Zhou Z, Wu L, Wang R, Papapetropoulos A, Szabo C. Hydrogen sulfide replacement therapy protects the vascular endothelium in hyperglycemia by preserving mitochondrial function. Proc Natl Acad Sci USA. 2011; 108:13829–13834. [PubMed: 21808008]
27. Wen YD, Wang H, Kho SH, Rinkiko S, Sheng X, Shen HM, Zhu YZ. Hydrogen sulfide protects HUVECs against hydrogen peroxide induced mitochondrial dysfunction and oxidative stress. PLoS One. 2013; 8:e53147. [PubMed: 23393548]
28. Tomasova L, Pavlovicova M, Malekova L, Misak A, Kristek F, Grman M, Cacanyiova S, Tomasek M, Tomaskova Z, Perry A, Wood ME, Lacinova L, Ondrias K, Whiteman M. Effects of AP39, a novel triphenylphosphonium derivatised anethole dithiolethione hydrogen sulfide donor, on rat haemodynamic parameters and chloride and calcium Cav3 and RyR2 channels. Nitric Oxide. 2015; 46:131–144. [PubMed: 25555533]
29. Ikeda K, Marutani E, Hirai S, Wood ME, Whiteman M, Ichinose F. Mitochondria-targeted hydrogen sulfide donor AP39 improves neurological outcomes after cardiac arrest in mice. Nitric Oxide. 2015 In press.
30. Marques VP, Gonçalves GM, Feitoza CQ, Cenedeze MA, Fernandes Bertocchi AP, Damião MJ, Pinheiro HS, Antunes Teixeira VP, dos Reis MA, Pacheco-Silva A, Saraiva Câmara NO. Influence of TH1/TH2 switched immune response on renal ischemia-reperfusion injury. Nephron Exp Nephrol. 2006; 104:e48–e56. [PubMed: 16741373]
31. Daemen MA, van't Veer C, Wolfs TG, Buurman WA. Ischemia/reperfusion-induced IFN-gamma up-regulation: involvement of IL-12 and IL-18. J Immunol. 1999; 162:5506–5510. [PubMed: 10228031]
32. Köken T, Serteser M, Kahraman A, Akbulut G, Dilek ON. Which is more effective in the prevention of renal ischemia-reperfusion-induced oxidative injury in the early period in mice: interleukin (IL)-10 or anti-IL-12? Clin Biochem. 2004; 37:50–55. [PubMed: 14675562]
33. Tripatara P, Patel NS, Collino M, Gallicchio M, Kieswich J, Castiglia S, Benetti E, Stewart KN, Brown PA, Yaqoob MM, Fantozzi R, Thiemermann C. Generation of endogenous hydrogen sulfide by cystathionine gamma-lyase limits renal ischemia/reperfusion injury and dysfunction. Lab Invest. 2008; 88:1038–1048. [PubMed: 18679378]
34. Simon F, Scheuerle A, Gröger M, Stahl B, Wachter U, Vogt J, Speit G, Hauser B, Möller P, Calzia E, Szabo C, Schelzig H, Georgieff M, Radermacher P, Wagner F. Effects of intravenous sulfide during porcine aortic occlusion-induced kidney ischemia/reperfusion injury. Shock. 2011; 35:156–163. [PubMed: 20661185]

35. Koning AM, Frenay AR, Leuvenink HG, van Goor H. Hydrogen sulfide in renal physiology, disease and transplantation-the smell of renal protection. Nitric Oxide. 2015; 46:37–49. [PubMed: 25656225]

Abbreviations

AOAA	aminooxyacetic acid
AP39	(10-oxo-10-(4-(3-thioxo-3H-1,2-dithiol-5yl) phenoxy)decyl) triphenylphosphonium bromide
ARF	acute renal failure
CBS	cystathionine-β-synthase (CBS)
CSE	cystathionine-γ-lyase
DCF	dichlorofluorescein
GOx	glucose oxidase
H_2O_2	hydrogen peroxide
H_2S	hydrogen sulfide
I/R	ischemia/reperfusion
3-MST	3-mercaptopyruvate sulfurtransferase

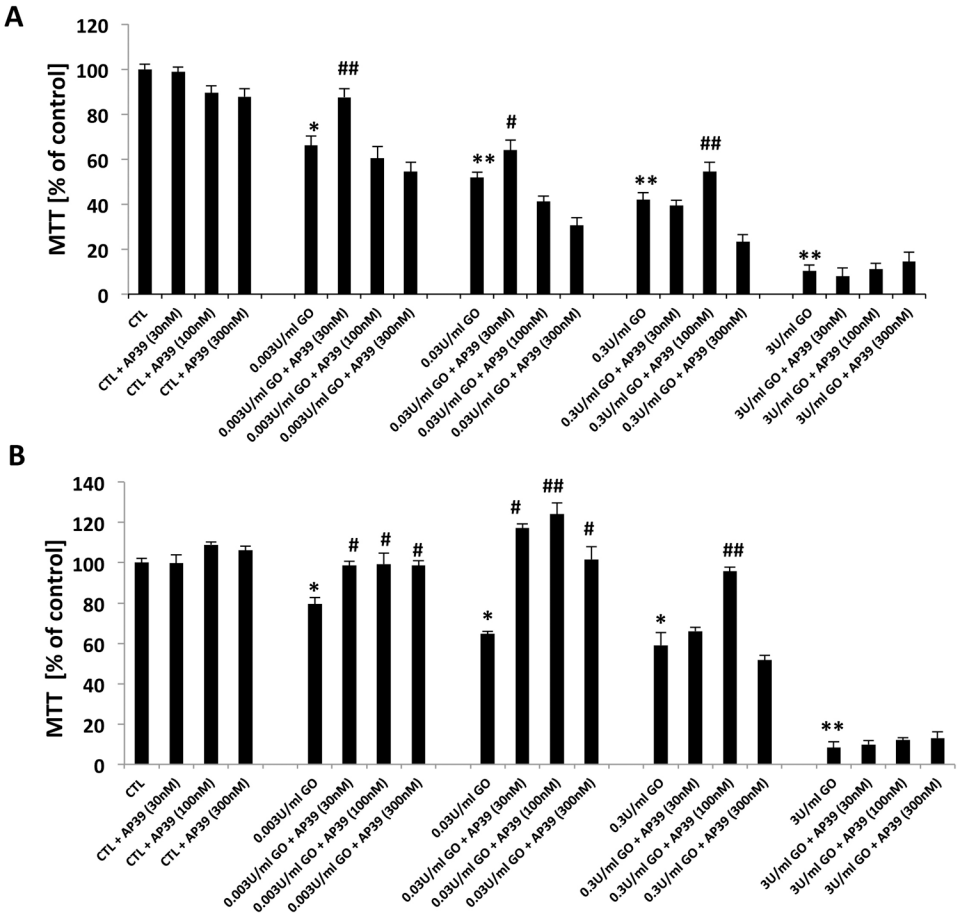

Figure 1. Effect of AP39 on the viability of oxidatively stressed NRK cells

AP39 (30 nM, 100 nM or 300 nM) pretreatment enhances cellular recovery after 1h (A) & 24h (B) of GOx exposure (0.003, 0.03, 0.3 or 3U/ml) on NRK cells, followed by the measurement of MTT conversion. There is a decrease in MTT conversion in GOx treated cells; these effects are attenuated by AP39. Data (% of vehicle-treated control values) are shown as mean ± SEM values from three independent experiments with 4–8 replicates for each end-point. * $p<0.05$, ** $p<0.01$ shows a significant decrease in MTT in response to GOx treatment (in the GOx treated group that also received AP39 vehicle, compared to the to baseline control in the absence of GOx or AP39). # $p<0.05$, ## $p<0.01$ shows a significant enhancement of MTT by AP39, when compared to its vehicle control in the presence of the same concentration of GOx.

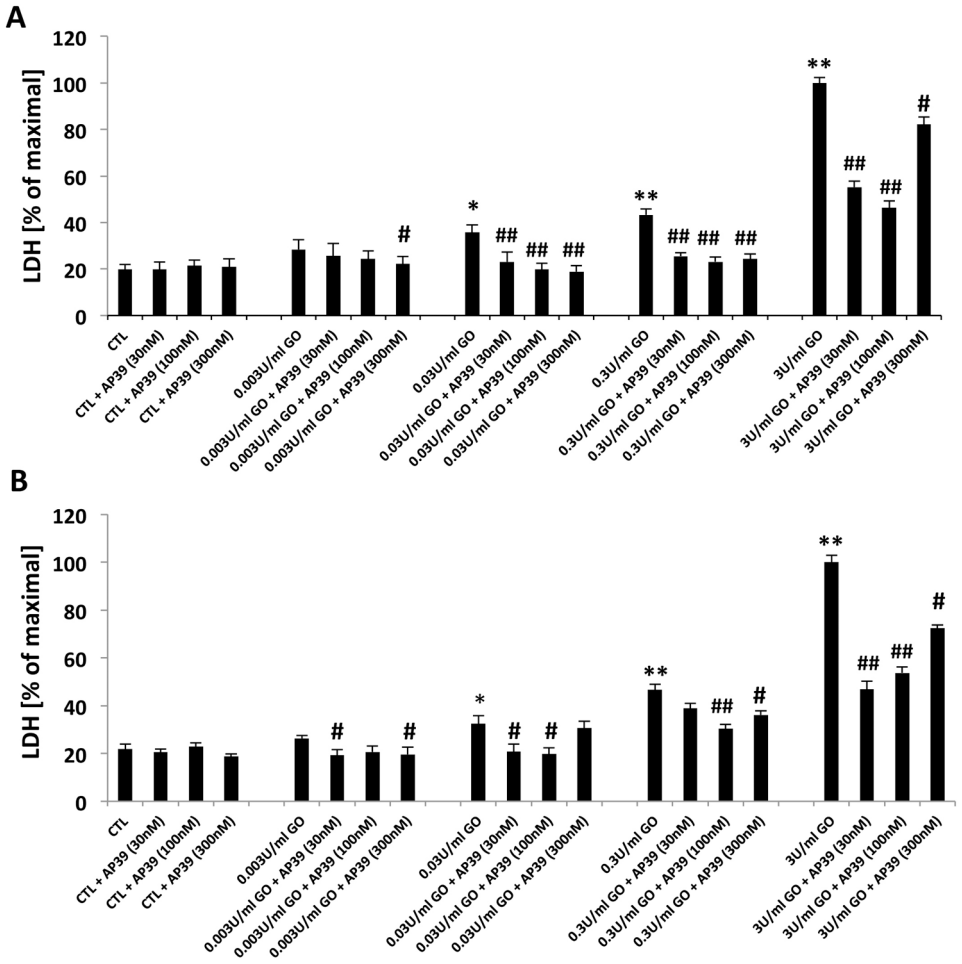

Figure 2. Effect of AP39 on LDH release of oxidatively stressed NRK cells

Cells were exposed to glucose oxidase (0.003, 0.03, 0.3 or 3U/ml) for 1h (A), in another set exposed to 1h followed by a washout and replacement of the medium with fresh tissue culture medium and incubated for a subsequent 24h (B), followed by the measurement of LDH conversion. There is an increase in LDH content of the medium of GOx treated cells; these effects are attenuated by AP39 (30 nM, 100 nM and 300 nM). Data are shown as mean ± SEM values from three independent experiments with 4–8 replicates for each end-point; values are expressed as the maximum LDH release observed at 3 U/ml GOx. * $p<0.05$, ** $p<0.01$ shows a significant increase in LDH release in response to GOx treatment (in the GOx treated group that also received AP39 vehicle, compared to the to baseline control in the absence of GOx or AP39). # $p<0.05$, ## $p<0.01$ shows a significant reduction of LDH by AP39, when compared to its vehicle control at the same concentration of GOx.

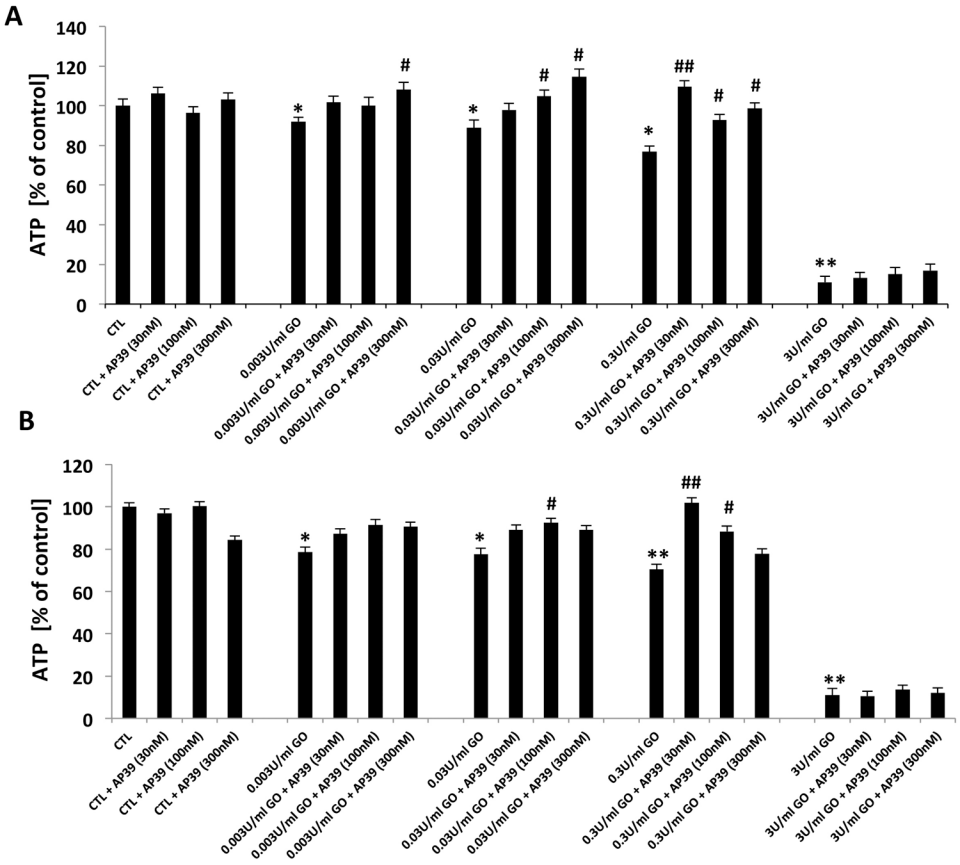

Figure 3. Effect of AP39 on cellular ATP levels of oxidatively stressed NRK cells

NRK cells were subjected to 1h (A) and 24h (B) GOx exposure (0.003, 0.03, 0.3& 3U/ml). Cells were pretreated with AP39 (30 nM, 100 nM or 300 nM) 30 min prior to GOx exposure. AP39-mediated protection was observed at intermediate concentrations of GOx. Data (% of vehicle-treated control values) are shown as mean ± SEM values from three independent experiments with 4–8 replicates for each end-point. * $p<0.05$, ** $p<0.01$ shows a significant decrease in ATP levels in response to GOx treatment, (in the GOx treated group that also received AP39 vehicle, compared to the to baseline control in the absence of GOx or AP39). # $p<0.05$, ## $p<0.01$ shows a significant enhancement of ATP levels by AP39, when compared to its corresponding control at the same concentration of GOx.

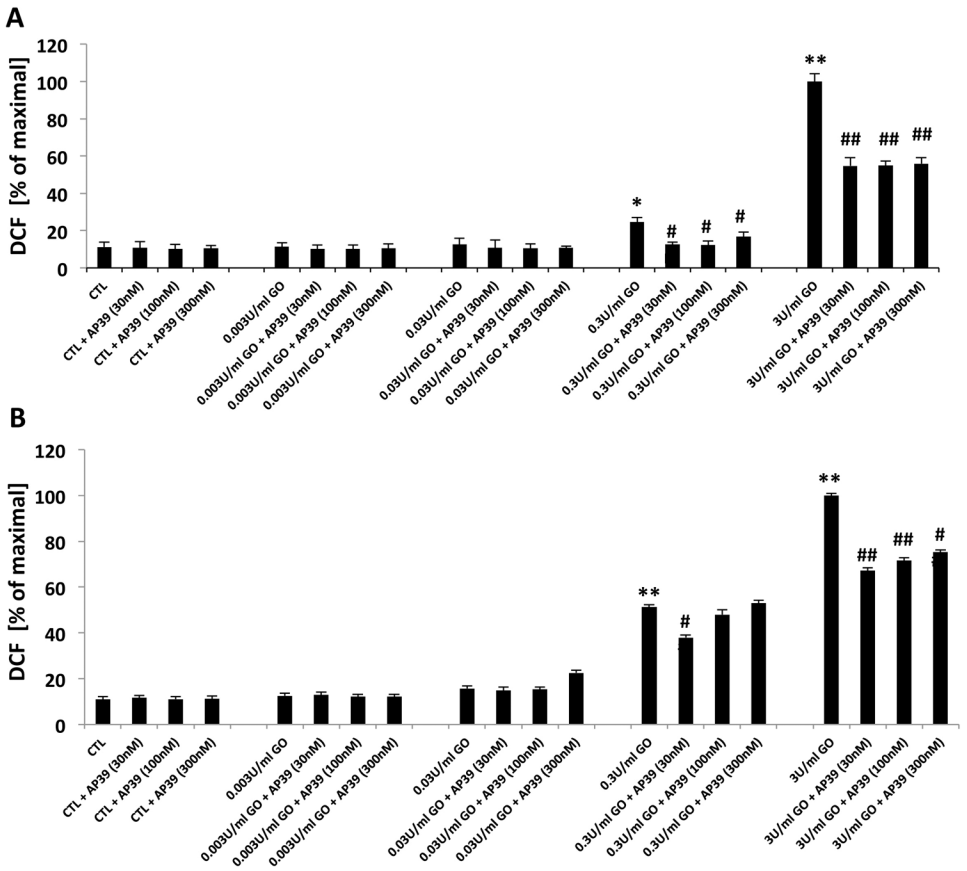

Figure 4. Effect of AP39 on DCF production of oxidatively stressed NRK cells

Increase in DCF fluorescence in response to exposure of GOx for 1h (A) and 24h (B) incubation in tissue culture medium of NRK cells is shown. Pretreatment with AP39 30 min prior to GOx exposure observed concentration dependent protective effect. Data are shown as mean ± SEM values from three independent experiments with 4–8 replicates for each end-point; values are expressed as the maximum DCF production observed at 3 U/ml GOx. * $p<0.05$, ** $p<0.01$ shows a significant increase in DCF fluorescence in response to GOx treatment, when compared to baseline control (in the absence of GOx or AP39). # $p<0.05$, ## $p<0.01$ shows a significant reduction of DCF fluorescence by AP39, when compared to its corresponding control at the same concentration of GOx.

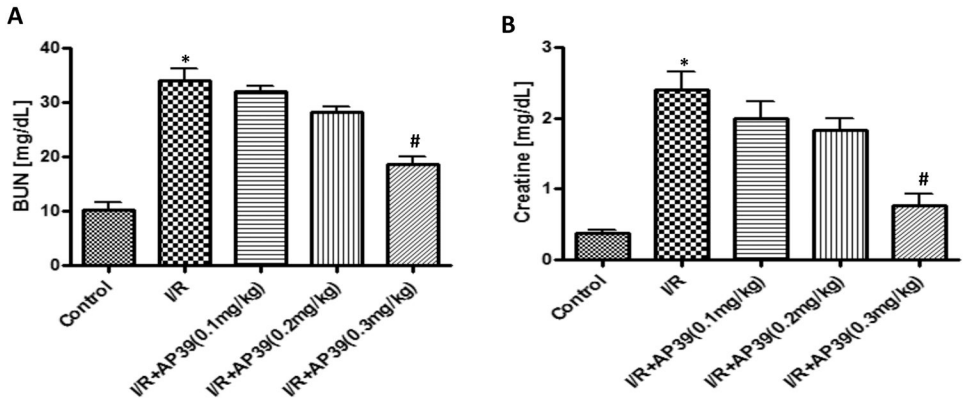

Figure 5. Effect of AP39 on BUN and creatinine plasma levels in a renal ischemia-reperfusion model in the rat

Renal I/R significantly impaired glomerular function, as evidenced by markedly increased (over 4-fold over sham control baseline) blood urea nitrogen (A) and creatinine levels (B); this increase was concentration-dependently reduced by AP39; most pronouncedly at the 0.3 mg/kg dose of the H_2S donor. Data are shown as mean ± SEM of 10 animals; *$p<0.05$ show significant increases in the vehicle-treated I/R group, compared to the sham control; # $p<0.05$ shows a significant protective effect of AP39 in I/R compared to the I/R group treated with AP39 vehicle.

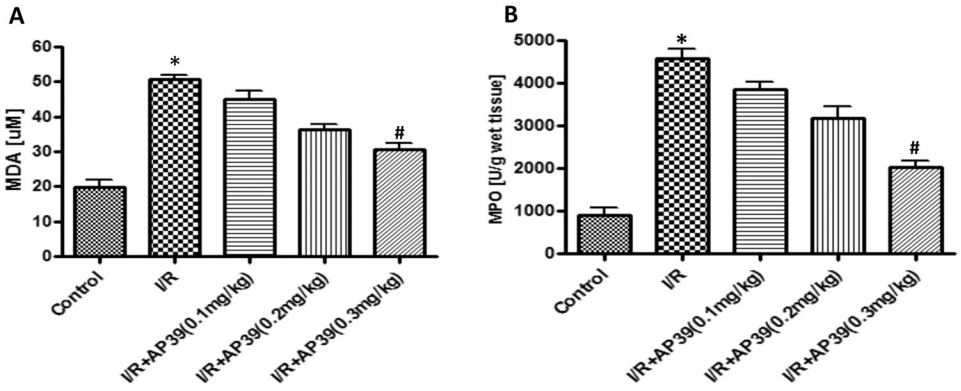

Figure 6. Effect of AP39 on MPO and MDA levels in a renal ischemia-reperfusion model in the rat

Renal I/R significantly increased renal MPO (A) and renal MDA levels (B); this increase was concentration-dependently reduced by AP39; most pronouncedly at the 0.3 mg/kg dose of the H_2S donor. Data are shown as mean ± SEM of 10 animals; *$p<0.05$ show significant increases in the vehicle-treated I/R group, compared to the sham control; # $p<0.05$ shows a significant protective effect of AP39 in I/R compared to the I/R group treated with AP39 vehicle.

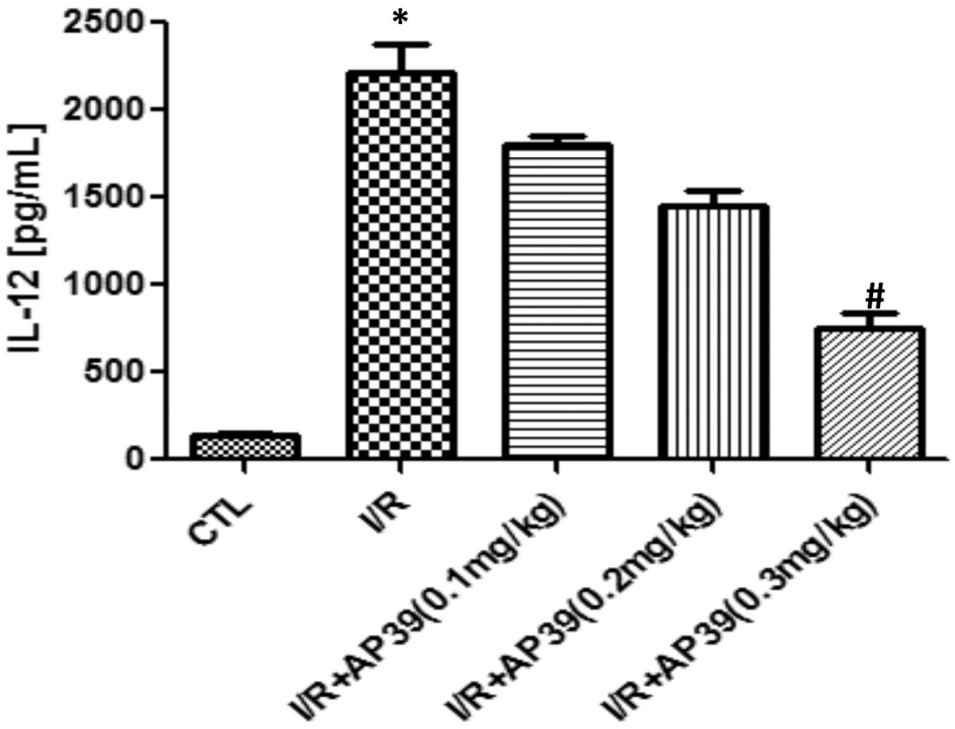

Figure 7. Effect of AP39 on plasma IL-12 levels in a renal ischemia-reperfusion model in the rat

Renal I/R significantly increased plasma IL-12 levels; this increase was concentration-dependently reduced by AP39; most pronouncedly at the 0.3 mg/kg dose of the H_2S donor. Data are shown as mean ± SEM of 10 animals; *$p<0.05$ show significant increases in the vehicle-treated I/R group, compared to the sham control; # $p<0.05$ shows a significant protective effect of AP39 in I/R compared to the I/R group treated with AP39 vehicle. Data are shown as mean ± SEM of 10 animals.

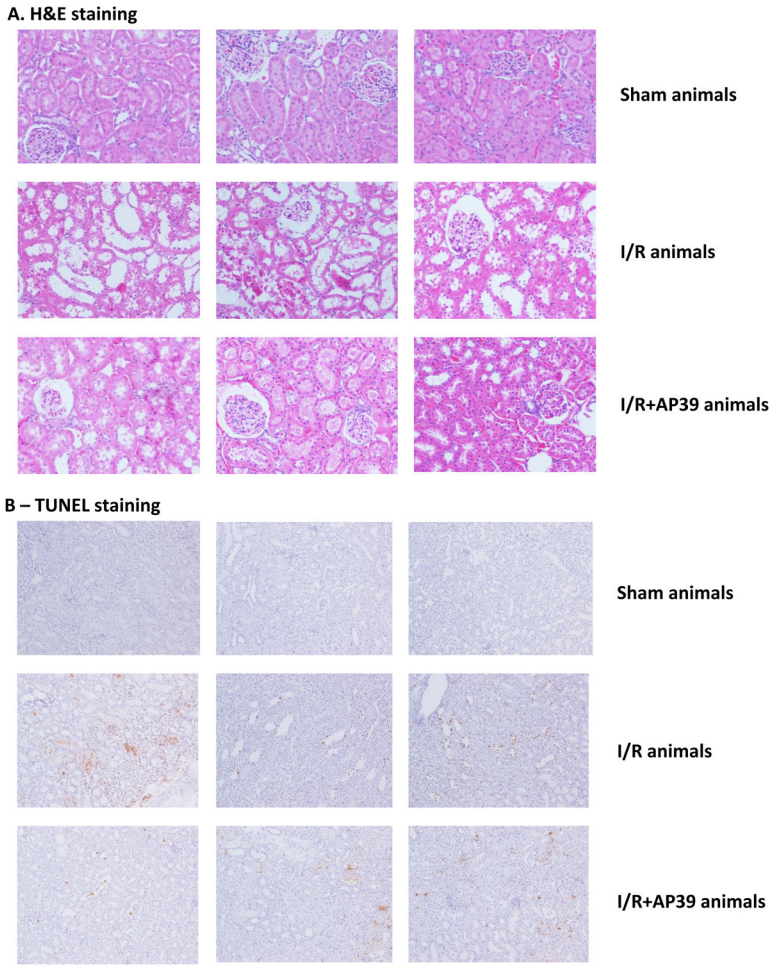

Figure 8. Effect of AP39 on histopathology and apoptosis in a renal ischemia-reperfusion model in the rat

Hematoxylin and eosin–stained sections are from the outer medulla are shown in (A); TUNEL staining is shown in (B). Top figures represent representative sham controls; middle figures represent vehicle-treated rats subjected to renal I/R; bottom figures represent an AP39 (0.3 mg/kg) treated rat subjected to renal I/R. Please note that neutrophil accumulation within the interstitium of the kidney, as well as the intensity of TUNEL staining was significantly reduced by AP39, but neither the histological damage, nor the TUNEL staining was completely normalized by AP39 treatment. Each group shows 3 representative animals of n=10 animals.